IEEE Photonics Journal
An IEEE Photonics Society Publication

Optimization Studies of Two-Phosphor-Coated White Light-Emitting Diodes

Volume 5, Number 2, April 2013

Ziquan Guo
Tienmo Shih
Yulin Gao
Yijun Lu
Lihong Zhu
Guolong Chen
Yue Lin
Jihong Zhang
Zhong Chen

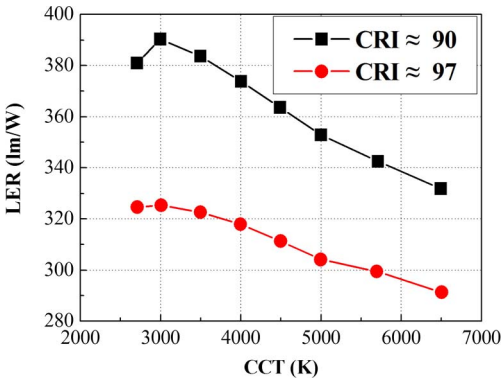

DOI: 10.1109/JPHOT.2013.2245885
1943-0655/$31.00 ©2013 IEEE

IEEE photonics SOCIETY

IEEE

Optimization Studies of Two-Phosphor-Coated White Light-Emitting Diodes

Ziquan Guo, Tienmo Shih, Yulin Gao, Yijun Lu, Lihong Zhu, Guolong Chen, Yue Lin, Jihong Zhang, and Zhong Chen

Department of Electronic Science, Fujian Engineering Research Center for Solid-state Lighting, State Key Laboratory of Physical Chemistry of Solid Surfaces, Xiamen University, Xiamen 361005, China

DOI: 10.1109/JPHOT.2013.2245885
1943-0655/$31.00 ©2013 IEEE

Manuscript received January 27, 2013; accepted January 31, 2013. Date of publication February 8, 2013; date of current version February 27, 2013. This work was supported in part by the Major Science and Technology Project between University-Industry Cooperation in Fujian Province under Grant 2011H6025, by the NNSF of China under Grant 11104230, and by the Key Project of Fujian Province under Grant 2012H0039. Corresponding authors: Y. Lu and Z. Chen (e-mail: yjlu@xmu.edu.cn; chenz@xmu.edu.cn).

Abstract: Three-hump InGaN-based white light-emitting diodes (LEDs) precoated with traditional yellow/green phosphors and red-emitting quantum dots (QDs), have been numerically investigated. Under variations of eight correlated color temperatures (CCTs), three wavelengths, two bandwidths, and two peak heights, optimal results of luminous efficacy radiation (LER) and color rendering index (CRI) are identified and retained through filtering off billions of unqualified candidates. These results include LER $= 390$ lm/W and CRI $= 90$ [chromaticity difference $(D_{uv}) < 0.0054$] at CCT $= 3000$ K. In addition, our photometric and colorimetric sensitivity studies provide the dependence of LER, CRI, CCT, and D_{uv} on LED spectral parameters affected by operating temperatures. Finally, we have discovered that higher instabilities may be induced for cool white LEDs (CCT $= 6500$ K) than for warm white LEDs (CCT $= 3000$ K) within the analysis of CCT versus spectral parameters.

Index Terms: Solid-state lighting, light-emitting diodes (LEDs), color rendering index (CRI), luminous efficacy of radiation.

1. Introduction

The light-emitting diode (LED) technology is regarded as one of the most promising inventions in past decades and may replace conventional incandescent and fluorescent lamps in the future. After the introduction of InGaN-based blue LEDs, the white LEDs fabricated by combining the blue LED with the Ce^{3+}-doped yttrium aluminum garnet (YAG: Ce^{3+}) have drawn wide attention due to their compact sizes, long life spans, low energy consumption, and especially high efficiencies [1], [2]. The development of phosphor-converted white (pc-W) LEDs is strongly spurred by the advances in high-efficiency III-Nitride-based pump LEDs [3]–[9]. The progress in high-efficiency nitride LED has been performed by various methods to suppress the charge separation issues in active regions [3]–[6] and reduce the dislocation density in materials [7]–[9]. In recent years, a great amount of effort has been devoted to improve the performance of pc-W LEDs by choosing proper phosphor materials and structures [10]–[12].

In 2012, LED lighting leader, Cree Inc., reported a barrier-breaking 254-lm/W [luminous efficacy (LE)] white LED [13]. LE of radiation (LER, K_e) and LE are related to each other via power conversion efficiency (PCE), i.e., $LE = LER \times PCE$ [14]. For a given PCE, a high LE requires a

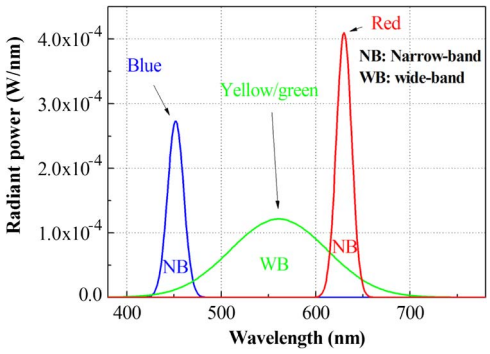

Fig. 1. SPDs of three humps.

high LER. However, color rendering index (CRI; R_a) is also a critical criterion for evaluating the performance of pc-W LEDs. In general, increases of LER lead to decreases of CRI [15]. Consequently, optimization procedures involving parametric values of LER and CRI will prove essential. In 1971, Thornton investigated the luminous and color-rendering performances of three-hump spectral power distribution (SPD) [16]. Three optimal wavelengths, i.e., 450 nm, 540 nm, and 610 nm, were proposed. In [15], analyses of two to five humps, including LER and CRI tradeoffs, were studied at correlated color temperature (CCT; T_c) equal to 4870 K [17]. In their studies, LER and CRI values are 430 lm/W and 3 for two-hump LEDs, 366 lm/W and 85 for three humps, 332 lm/W and 98 for four humps, 324 lm/W and 99 for five humps, respectively. In 2009, Erdem *et al.* [18] explored four-hump white LEDs with CRI $>$ 90 and LER $>$ 380 lm/W, using nanocrystal quantum dots (QDs) at CCT $=$ 3000 K. Afterwards, QD hybridized white LEDs with high performance exhibiting a high LER $>$ 350 lm/W and a high CRI close to 90 at a low CCT $<$ 3000 K were experimentally investigated by the same group [19]. In [20], analyses of four-hump QD white LEDs at eight different CCTs were reported, yielding high values of LER. Recently, subjects related to QDs have drawn considerable attention due to favorable properties including tunable emission wavelengths, narrow bandwidths, and reasonable quantum efficiencies [14], [21].

In this paper, we have investigated three-hump SPDs emitted by InGaN-based white LEDs, using traditional yellow/green phosphors (such as YAG : Ce^{3+}) and red-emitting QDs. Our findings include the following: 1) comprehensive results for eight values of CCT; 2) a set of parametric values that are optimal for LED performances; 3) dependence of LER and CRI values on peak wavelength and full width at half-maximum (FWHM) affected by LED operating temperatures; and 4) trends that may be used as a reference for other numerical studies and laboratory experiments.

2. Analyses and Numerical Simulations

In our paper, we have selected spectra that exhibit three peaks at $\lambda_B = 430 - 490$ nm, $\lambda_{Y/G} = 500 - 590$ nm, and $\lambda_R = 600 - 660$ nm, as schematically shown in Fig. 1, indicating blue, yellow/green, and red colors. Typically, FWHM for blue chips is approximately 30 nm, while those of traditional phosphors and emerging QDs are located within 50–130 nm and 19–49 nm or wider [2], [14], [22], respectively.

The primary reason of selecting three-hump spectra is the simplicity. Because of this attribute, we are able to keep the number of varying parameters relatively low.

2.1. Modeling of Humps

The function of a single narrowband (NB) hump, shown in Fig. 1, follows the Gaussian distribution, defined as [23], [24]

$$E_{NB}(\lambda, \lambda_p, w_b) = \Phi(\lambda, \lambda_p, w_b) = \frac{1}{3}\left\{G(\lambda, \lambda_p, w_b) + 2\left[G(\lambda, \lambda_p, w_b)\right]^5\right\} \quad (1)$$

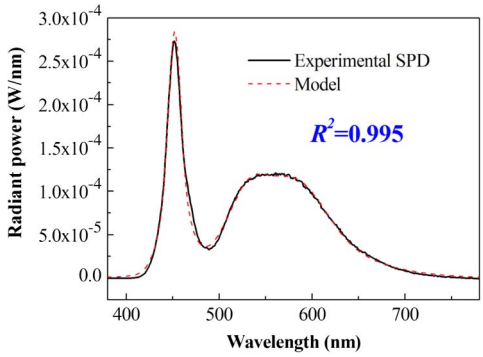

Fig. 2. Experimental SPDs vs. models.

where $G(\lambda, \lambda_p, w_b) = \exp[-(\lambda - \lambda_p)^2 / w_b^2]$. Parameters λ, λ_p, and w_b denote wavelength, peak wavelength, and FWHM, respectively.

The hump for the middle wideband (WB) can be adequately modeled by superimposing two humps, as described by

$$E_{WB}(\lambda, \lambda_p, w_b) = \Phi(\lambda, \lambda_{p1}, w_{b1}) + \Phi(\lambda, \lambda_{p1}, w_{b2}) \tag{2}$$

where $\lambda_{p1} = \lambda_p - a \cdot w_b$, $\lambda_{p2} = \lambda_p - b \cdot w_b$, $w_{b1} = c \cdot w_b$, and $w_{b2} = d \cdot w_b$. Symbols a, b, c, and d are fitting parameters. Consequently, the model of three-hump SPD can be given as

$$E(\lambda) = H_B \times E_{NB}(\lambda, \lambda_B, w_B) + H_{Y/G} \times E_{WB}(\lambda, \lambda_{Y/G}, w_{Y/G}) + H_R \times E_{NB}(\lambda, \lambda_R, w_R) \tag{3}$$

where λ_B, $\lambda_{Y/G}$, λ_R, w_B, $w_{Y/G}$, w_R, H_B, $H_{Y/G}$, and H_R represent the blue, yellow/green, and red peak wavelengths; blue, yellow/green, and red FWHMs; and blue, yellow/green, and red peak heights, respectively.

2.2. Experiments

In our laboratory, SPDs of white LEDs, which are emitted by an InGaN-based blue die and YAG : Ce^{3+}-based yellow/green phosphor, were measured by the SP320 spectrometer with an integration sphere manufactured by Instrument Systems Inc. During measurements, white LEDs were placed in a temperature-controlled oven maintained at the room temperature (300 K) under a dc of 20 mA. The temperature-controlled oven is used to warrant the constancy of ambient temperature. Fig. 2 shows experimental SPDs versus models, which are nearly identical (with R-square $>$ 0.99). This model may also remain applicable to other phosphors, since their SPDs exhibit similar shapes of YAG-humps [25].

2.3. Definitions of Parameters

Prior to reporting the results, it is appropriate to define parameters including LER, CRI, and color quality scale (CQS; Q_a).

a) LER represents the ratio of optical power of emitted spectra perceived by human eyes to the emitted total optical power. It can be written as [14], [15]

$$K_e = \frac{683 \times \int_{380}^{780} E(\lambda) V(\lambda)\, d\lambda}{\int_0^{\infty} E(\lambda)\, d\lambda} (lm/W) \tag{4}$$

where $V(\lambda)$ is the CIE photopic eye sensitivity function.

TABLE 1

Ranges and increments of parametric values

Color	Wavelength (nm) $(\Delta\lambda = 1)$	FWHM (nm) $(\Delta w = 1)$	Peak height (mW) $(\Delta H = 0.001)$
Blue	430-490	30-30	0.273-0.273
Yellow/Green	500-590	50-130	0.100-1.500
Red	600-660	19-49	0.100-1.500

b) CRI is defined as the ability of reproducing the colors of various objects vividly by a light source [26], namely

$$R_i = 100 - 4.6\Delta E_i \tag{5}$$

$$R_a = \frac{1}{8}\sum_{i=1}^{8} R_i \tag{6}$$

where ΔE_i is the difference in color appearance for each of eight reflective samples $(i = 1 - 8)$ illuminated by the test and the reference sources in the CIE 1964 $W^*U^*V^*$ uniform color space.

c) CQS, which attempts to rectify the shortcomings of the CRI, was proposed by the National Institute of Standards and Technology (NIST) and can be written as [27]

$$Q_{a,rms} = 100 - 3.1 \times \sqrt{\frac{1}{15}\sum_{i=1}^{15}\left(\Delta E^*_{ab,sat,i}\right)^2} \tag{7}$$

$$Q_{a,0-100} = 10\ln\left[\exp\left(\frac{1}{10}Q_{a,rms}\right) + 1\right] \tag{8}$$

$$Q_a = M_{CCT} \times Q_{a,0-100} \tag{9}$$

where $\Delta E^*_{ab,sat,i}$ is the color difference for each of 15 reflective samples $(i = 1 - 15)$ illuminated by the test and reference sources with the integration of the saturation factor in the CIE 1976 $L^*a^*b^*$ color space; M_{CCT} is the CCT factor [27].

2.4. Numerical Procedure

Clearly, there are three humps. Each hump is associated with three attributes, i.e., three peak wavelengths, three FWHMs, and three peak heights. Therefore, totally and theoretically, there are 3×3 attributes that can be varied. In our numerical simulations, however, realizing that the peak height (H_B exemplified as 0.273 mW measured in our laboratory) and FWHM (w_B) of blue LED can remain unaltered, we actually are able to reduce nine to seven. Ranges and increments ($\Delta\lambda$, Δw, and ΔH) of parametric values are shown in Table 1. The total number of simulations can be estimated by multiplying exact numbers of variations for these seven attributes. Methods of filtering are exemplified by the following: 1) CRI ≥ 90, CQS ≥ 80, CCT $- 10$ K $<$ 3000 K $<$ CCT $+ 10$ K, and color distance $(D_{uv}) < 0.0054$ [20], [26]; and 2) CRI ≥ 97, CQS ≥ 94, $R_9 \geq 94$ (the CIE special CRI of test color sample 9), CCT $- 10$ K $<$ 3000 K $<$ CCT $+ 10$ K, and $D_{uv} < 0.0054$. In achieving the goal of obtaining optimal LER values, it is worth considering various CCT values that are adopted to be 2700 K, 3000 K, 3500 K, 4000 K, 4500 K, 5000 K, 5700 K, and 6500 K [20], [24]. With billions of

TABLE 2

Peak wavelengths, FWHMs, peak heights, photometric and colorimetric performances with CRI $\geq$ 90 and CQS $\geq$ 80, CCT $-$ 10 K $<$ 3000 K $<$ CCT $+$ 10 K, and $D_{uv} < 0.0054$ at CCTs of 2700 K to 6500 K

Target CCT (K)	2700	3000	3500	4000	4500	5000	5700	6500
CCT (K)	2704	2998	3496	4003	4491	4995	5693	6493
D_{uv}	0.0026	0.0029	0.0044	0.0052	0.0048	0.0049	0.0051	0.0052
λ_B (nm)	464	461	461	458	458	456	456	456
$\lambda_{Y/G}$ (nm)	554	551	549	546	543	542	540	538
λ_R (nm)	617	617	617	617	615	616	614	612
w_B (nm)	30	30	30	30	30	30	30	30
$w_{Y/G}$ (nm)	69	69	69	69	69	69	69	69
w_R (nm)	19	19	19	19	19	19	19	19
H_B (mW)	0.273	0.273	0.273	0.273	0.273	0.273	0.273	0.273
$H_{Y/G}$ (mW)	0.410	0.464	0.364	0.310	0.257	0.232	0.200	0.176
H_R (mW)	1.338	1.311	0.865	0.656	0.514	0.423	0.337	0.279
CRI	90	90	90	90	91	91	91	91
CQS	81	80	80	81	83	83	82	82
R_9	21	27	36	46	37	51	37	25
LER (lm/W)	381	390	384	374	364	353	343	332

unqualified candidates eliminated [18], [19], filtered results are categorized into two groups: CRI $\approx$ 90 and CRI $\approx$ 97.

3. Results and Discussions

3.1. Optimal Results

Table 2 shows optimal LER values for CRI $\approx$ 90. At CCT $\approx$ 3000 K, the LER value is 390 lm/W, indicating the highest among all CCT values. In Table 3 for CRI $\approx$ 97, also at CCT $\approx$ 3000 K, the optimal LER is 325 lm/W. As CRI values increase, LER values decrease. In comparison, most R_9 values lie lower than 50 for CRI $\approx$ 90 but greater than 95 for CRI $\approx$ 97. Since LER values are critical, and these values in the former case are much higher than those in the latter, we recommend the former even though its R_9 values are low.

To summarize these two tables, we propose that a combination of LER $=$ 390 lm/W and CRI $=$ 90 under CCT $\approx$ 3000 K at $\lambda_B = 461$ nm, $\lambda_{Y/G} = 551$ nm, $\lambda_R = 617$ nm, $w_B = 30$ nm, $w_{Y/G} =$ 69 nm, and $w_R = 19$ nm (the smallest value for red QDs in our simulations is 19 nm) be adopted for three-hump SPDs. This finding is moderately comparable with the optimal result of LER $=$ 388 lm/W reported in [18], LER $=$ 408 lm/W in [2], and LER $=$ 401 lm/W in [20] for warm white four-hump SPD. Finally, these numerical parameters can be seen to fall in the range of achievable laboratory settings [2] and can be experimentally duplicated. If we collect some data for CCT $\approx$ 3000 K and CRI $\approx$ 90, Fig. 3 can be obtained to show the tradeoff trends between LER and CRI.

Fig. 4 shows two curves of LER versus CCT for CRI $\approx$ 90 and 97. It can be seen that peaks take place at CCT $\approx$ 3000 K. As expected, the curve for CRI $\approx$ 97 lies underneath that for CRI $\approx$ 90. In addition, at CCT $\approx$ 3000 K, the difference is 65, which is maximum among all CCT categories. However, at CCT $\approx$ 6500 K, the difference is 41, which is minimum.

TABLE 3

Peak wavelengths, FWHMs, peak heights, photometric and colorimetric performances with CRI $\geq$ 97 and CQS $\geq$ 94, $R_9 \geq 94$, CCT $-$ 10 K $<$ 3000 K $<$ CCT $+$ 10 K, and $D_{uv} < 0.0054$ at CCTs of 2700 K to 6500 K

Target CCT (K)	2700	3000	3500	4000	4500	5000	5700	6500
CCT (K)	2707	3007	3498	3995	4495	4995	5693	6502
D_{uv}	0.0004	0.0004	0.0002	0.0004	0.0007	0.0011	0.0010	0.0008
λ_B(nm)	461	460	459	457	456	455	454	453
$\lambda_{Y/G}$(nm)	569	564	561	555	553	549	544	540
λ_R(nm)	630	630	631	630	631	631	630	629
w_B(nm)	30	30	30	30	30	30	30	30
$w_{Y/G}$(nm)	130	130	130	130	130	130	130	130
w_R(nm)	30	30	30	30	30	30	30	30
H_B(mW)	0.273	0.273	0.273	0.273	0.273	0.273	0.273	0.273
$H_{Y/G}$(mW)	0.646	0.504	0.364	0.291	0.244	0.215	0.199	0.178
H_R(mW)	1.241	0.882	0.510	0.373	0.273	0.232	0.192	0.160
CRI	97	97	98	98	98	98	98	98
CQS	94	95	95	96	95	95	94	94
R_9	94	97	97	98	98	95	98	96
LER (lm/W)	324	325	323	318	311	304	300	291

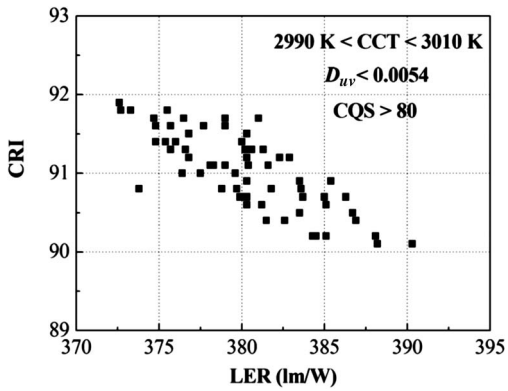

Fig. 3. Tradeoff trends of CRI and LER at CCT $\approx$ 3000 K and CRI $\approx$ 90.

In Fig. 5(a) and (b), optimal peak wavelengths versus CCT values are shown for CRI $\approx$ 90 and 97, respectively. It is interesting to note that the wavelengths for all three colors decrease as CCT value increases, prompting the recommendation that decreasing these λ values should be similarly performed. In the future, when conducting numerical simulations, we may be able to skip both numerical and laboratory experiments for unnecessary variations in different directions. Only at CRI $\approx$ 97, λ_R almost remains constant, implying that possibly numerical simulations can exclude variations of λ_R, saving some computation time. Finally, we observe that the decrease of $\lambda_{Y/G}$ is relatively rapid. This trend instructs us to choose finer resolutions of varying increments during numerical experiments.

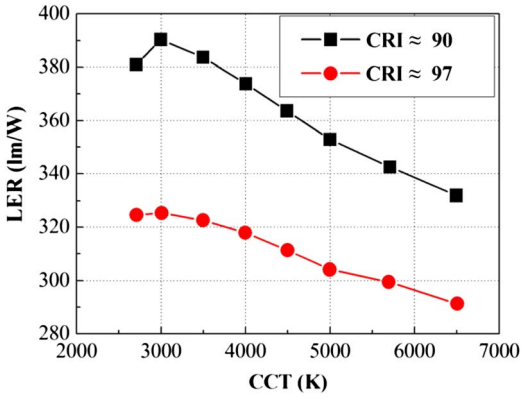

Fig. 4. LERs versus CCTs for CRI ≈ 90 and 97.

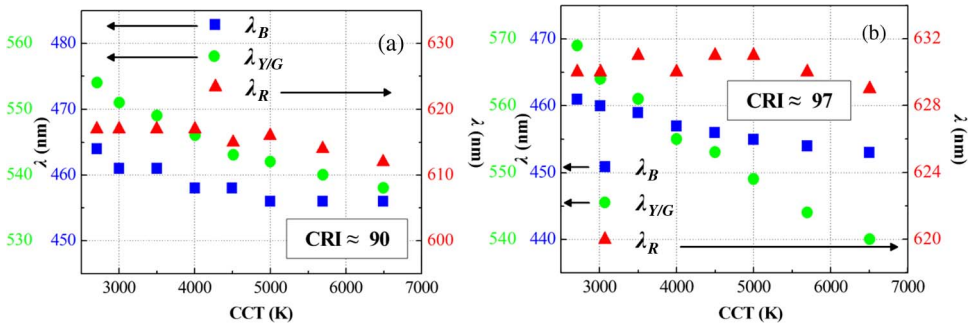

Fig. 5. Optimal peak wavelengths vs. CCTs at (a) CRI ≈ 90 and (b) CRI ≈ 97.

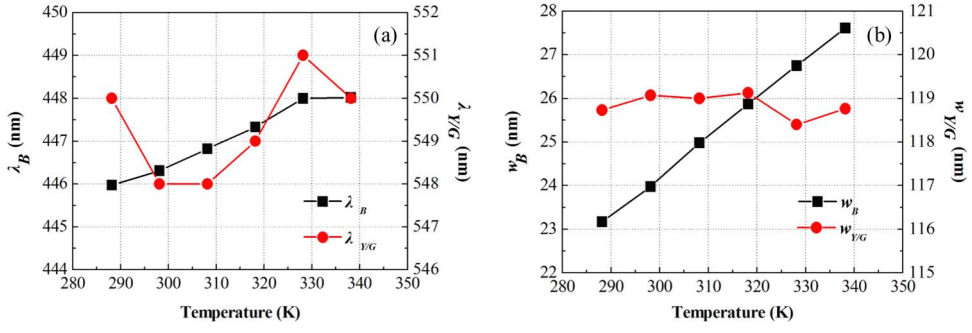

Fig. 6. Experimental peak wavelengths and FWHMs of (a) InGaN-based blue chip and (b) YAG : Ce^{3+}-based yellow/green phosphor vs. the ambient temperature.

3.2. Photometric and Colorimetric Sensitivity Studies

In reality, operating junction temperatures of LED will shift during operating lifetimes. This shift will affect SPDs of three-hump LEDs, which subsequently will affect LER and CRI values among others [2], [21], [28]. Therefore, some more analyses that investigate the sensitivity of LER, CRI, CCT, and D_{uv} against spectral parameters such as peak wavelength and FWHM are warranted.

Fig. 6(a) and (b) shows the measurements of peak wavelength and FWHM versus ambient temperature, conducted in our laboratory. It can be seen that the variations of all parameters, i.e., λ_B, $\lambda_{Y/G}$, w_B, and $w_{Y/G}$, are confined in 5 nm from 288 K to 338 K. Under similar temperature

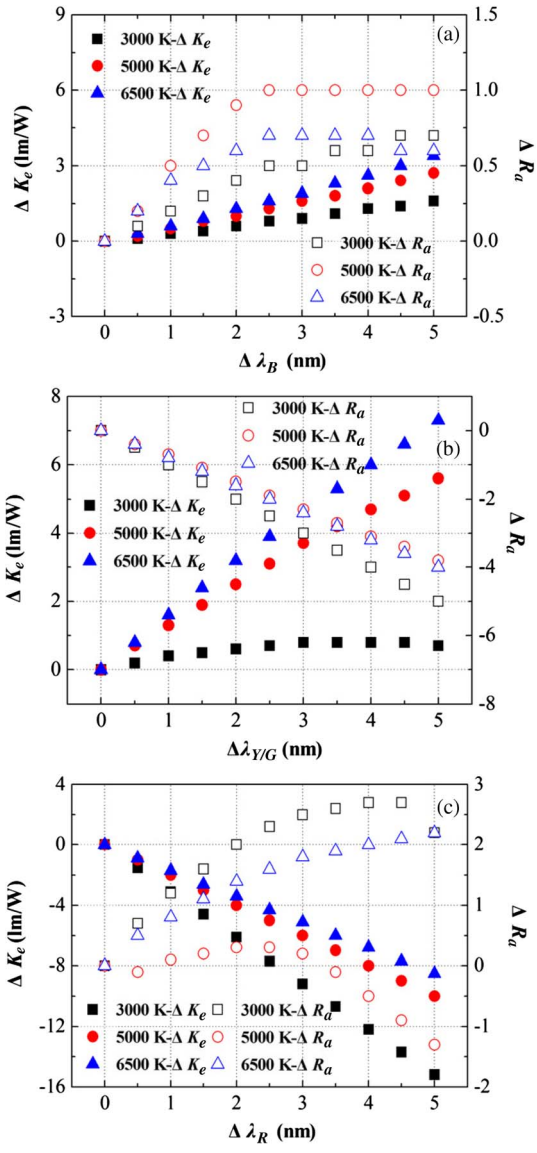

Fig. 7. ΔK_e and ΔR_a versus the deviation of peak wavelengths. (a) Blue, (b) yellow/green, and (c) red.

ranges, peak wavelength and FWHM of QDs (λ_R and w_R) also vary for approximately 5 nm [21], [29], guiding us to adopt the same variations in our numerical simulations.

In this paper, the deviations of LER, CRI, CCT, peak wavelengths, and FWHMs can be defined as

$$\Delta x = x - x_0 (x = K_e, R_a, T_c, \lambda_B, \lambda_{Y/G}, \lambda_R, w_B, w_{Y/G}, \text{ and } w_R) \tag{10}$$

where x_0 represents the reference (i.e., optimal) value of x. Also, the color distance between the arbitrary point (u, v) and reference point (u_0, v_0) on the 1960 UV chromaticity diagram can be given as

$$\Delta uv = \sqrt{\left[(u-u_0)^2 + (v-v_0)^2\right]}. \tag{11}$$

In the sensitivity studies, we take the optimal SPDs of CRI $\approx$ 90 under CCT $\approx$ 3000 K, 5000 K, and 6500 K as our nominal cases (shown in Table 2, third, seventh, and ninth columns). Fig. 7

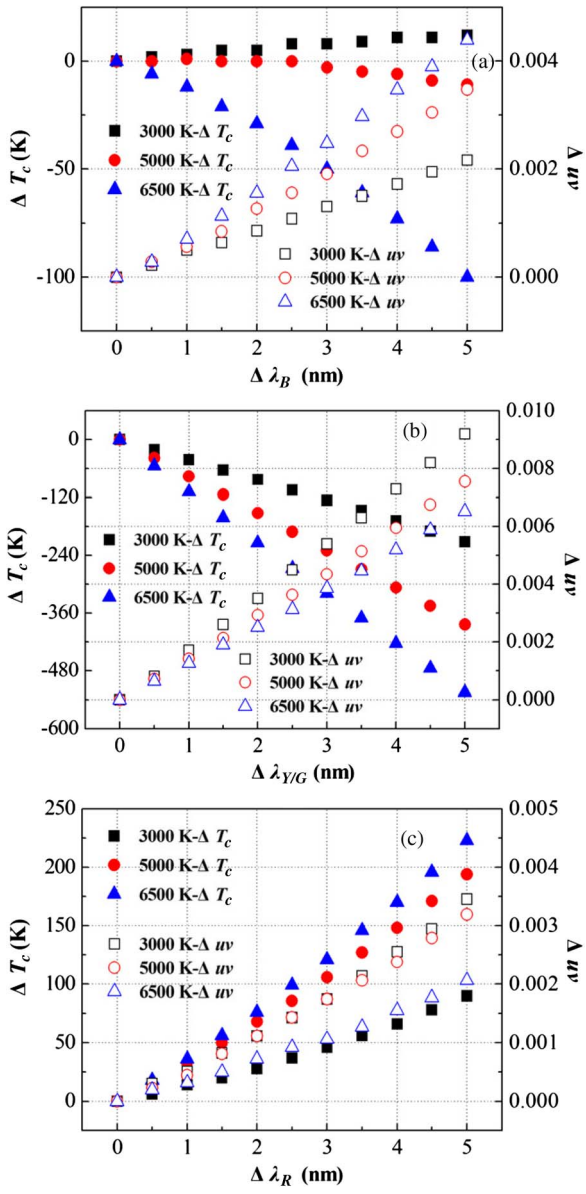

Fig. 8. ΔT_c and Δuv versus the deviation of peak wavelengths. (a) Blue, (b) yellow/green, and (c) red.

shows ΔK_e and ΔR_a versus the deviation of peak wavelengths. In Fig. 7(a), as the deviation of blue wavelength increases, both LER and CRI values are observed to increase under three different CCT conditions. Although these increases appear more desirable than the optimized condition identified in Table 2 (third, seventh, and ninth columns), those CRI, CQS, CCT, and D_{uv} values may lie beyond filtering ranges (CRI $\geq$ 90, CQS $\geq$ 80, CCT $-$ 10 K $<$ 3000 K, 5000 K, and 6500 K $<$ CCT $+$ 10 K, and $D_{uv} < 0.0054$). For example, under CCT $\approx$ 3000 K, D_{uv} values have been found to be larger than 0.0054 for $\Delta\lambda_B > 1$ nm. Similarly, in Fig. 7(b) and (c), these facts that CRI, CQS, CCT, and D_{uv} values also lie beyond filtering ranges have been checked and confirmed.

In Fig. 8(a)–(c), we plot ΔT_c and Δuv versus the deviation of peak wavelengths. For all wavelengths, maximum changes of CCT values take place at CCT $\approx$ 6500 K, suggesting that highest instabilities may be induced due to changes of peak wavelengths for cool white LEDs. Based on Fig. 8(a) and (b), most CCT values decrease as $\Delta\lambda_B$ or $\Delta\lambda_{Y/G}$ increases, except that CCT increases along with $\Delta\lambda_B$ for the optimal case of CCT $\approx$ 3000 K. Also, CCT values increase as

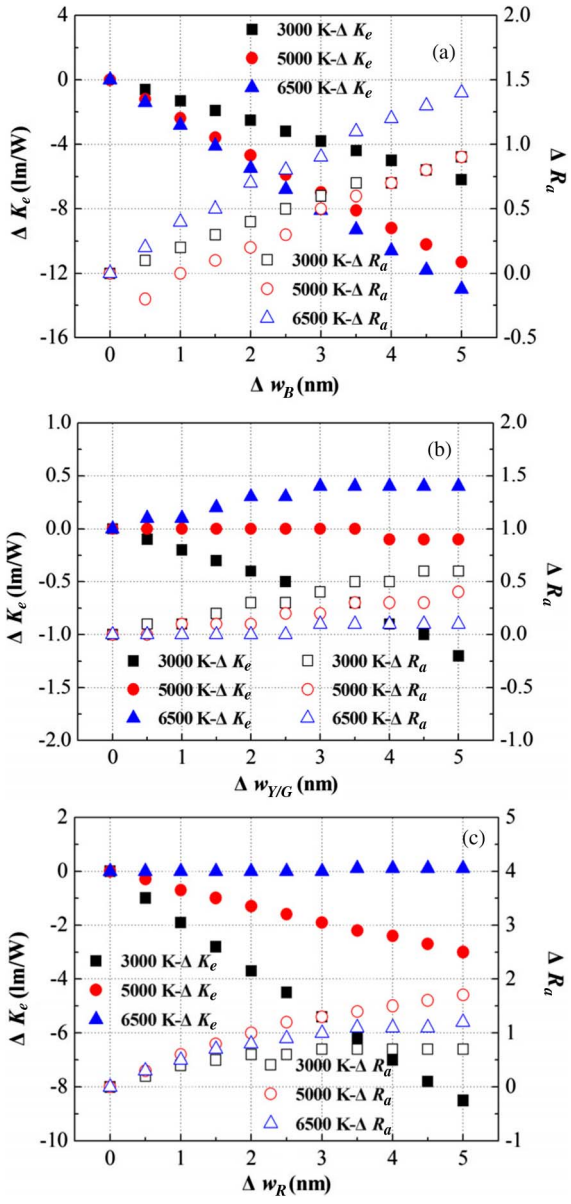

Fig. 9. ΔK_e and ΔR_a versus the deviation of FWHMs. (a) Blue, (b) yellow/green, and (c) red.

$\Delta\lambda_R$ increases, as found in Fig. 8(c). Fig. 9(a)–(c) exhibits LER and CRI behaviors versus the deviation of FWHMs. Of particular interest is Fig. 9(b), where we observe little variations of both LER and CRI for the case of $w_{Y/G}$, indicating that we may consider neglecting parametric variations for $w_{Y/G}$ for designing conveniences. Finally, in Fig. 10(a)–(c), we show ΔT_c and Δuv versus the deviation of FWHMs. Similarly, largest changes of CCT values occur at CCT $\approx$ 6500 K for all FWHMs.

4. Conclusion

In this paper, three-hump SPDs emitted by white LEDs have been considered, and comprehensive numerical simulations have been performed under eight CCT values and two CRI threshold values. Experiments have been conducted to provide SPD models. We have found that, at CCT $\approx$ 3000 K, optimal values of LER and CRI are 390 lm/W and 90, respectively. For the sake of rigorousness, photometric and colorimetric sensitivity analyses have been performed to show that

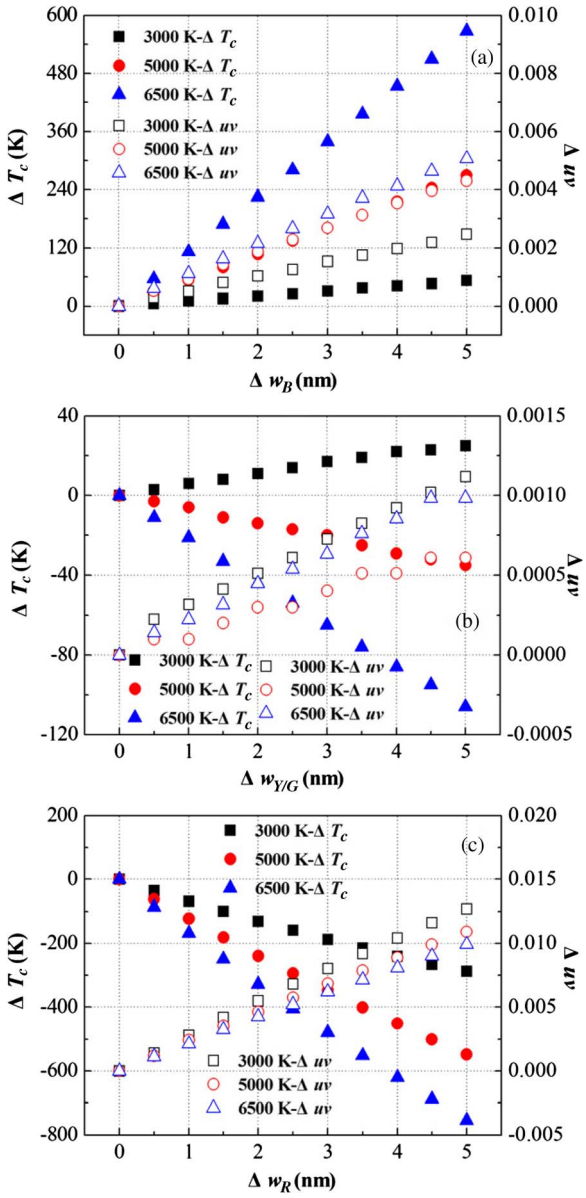

Fig. 10. ΔT_c and Δuv versus the deviation of FWHMs. (a) Blue, (b) yellow/green, and (c) red.

CRI, CQS, CCT, and D_{uv} lie beyond the filtering range (CRI $\geq$ 90, CQS $\geq$ 80, CCT $-$ 10 K $<$ 3000 K, 5000 K and 6500 K $<$ CCT + 10 K, and D_{uv} $<$ 0.0054) as the deviations of spectral parameters, i.e., peak wavelengths and FWHMs, vary from 0 to 5 nm. The changes of LER, CRI, CCT, and D_{uv} have been observed to be associated with the shifts of peak wavelengths and FWHMs affected by LED operating temperatures.

References

[1] E. F. Schubert and J. K. Kim, "Solid-state light sources getting smart," *Science*, vol. 308, no. 5726, pp. 1274–1278, May 2005.

[2] J. M. Phillips, M. F. Coltrin, M. H. Crawford, A. J. Fischer, M. R. Krames, R. Mueller-Mach, G. O. Mueller, Y. Ohno, L. E. S. Rohwer, J. A. Simmons, and J. Y. Tsao, "Research challenges to ultra-efficient inorganic solid-state lighting," *Laser Photon. Rev.*, vol. 1, no. 4, pp. 307–333, Dec. 2007.

[3] R. M. Farrell, E. C. Young, F. Wu, S. P. DenBaars, and J. S. Speck, "Materials and growth issues for high-performance nonpolar and semipolar light-emitting devices," *Semicond. Sci. Technol.*, vol. 27, no. 2, pp. 024001-1–024001-14, Feb. 2012.
[4] I. L. Koslow, M. T. Hardy, P. S. Hsu, P.-Y. Dang, F. Wu, A. Romanov, Y.-R. Wu, E. C. Young, S. Nakamura, J. S. Speck, and S. P. DenBaars, "Performance and polarization effects in (112) long wavelength light emitting diodes grown on stress relaxed InGaN buffer layers," *Appl. Phys. Lett.*, vol. 101, no. 12, pp. 121106-1–121106-4, Sep. 2012.
[5] H. Zhao, G. Liu, J. Zhang, J. D. Poplawsky, V. Dierolf, and N. Tansu, "Approaches for high internal quantum efficiency green InGaN light-emitting diodes with large overlap quantum wells," *Opt. Exp.*, vol. 19, no. S4, pp. A991–A1007, Jul. 2011.
[6] J. Zhang and N. Tansu, "Improvement in spontaneous emission rates for InGaN quantum wells on ternary InGaN substrate for light-emitting diodes," *J. Appl. Phys.*, vol. 110, no. 11, pp. 113110-1–113110-5, Dec. 2011.
[7] Y.-K. Ee, J. M. Biser, W. Cao, H. M. Chan, R. P. Vinci, and N. Tansu, "Metal organic vapor phase epitaxy of III-nitride light-emitting diodes on nano-patterned AGOG sapphire substrate by abbreviated growth mode," *IEEE J. Sel. Topics Quantum Electron.*, vol. 15, no. 4, pp. 1066–1072, Jul./Aug. 2009.
[8] Y.-K. Ee, X.-H. Li, J. Biser, W. Cao, H. M. Chan, R. P. Vinci, and N. Tansu, "Abbreviated MOVPE nucleation of III-nitride light-emitting diodes on nano-patterned sapphire," *J. Cryst. Growth*, vol. 312, no. 8, pp. 1311–1315, Apr. 2010.
[9] Y. Li, S. You, M. Zhu, L. Zhao, W. Hou, T. Detchprohm, Y. Taniguchi, N. Tamura, S. Tanaka, and C. Wetzel, "Defect-reduced green GaInN/GaN light-emitting diode on nanopatterned sapphire," *Appl. Phys. Lett.*, vol. 98, no. 15, pp. 151102-1–151102-3, Apr. 2011.
[10] H.-C. Kuo, C.-W. Hung, H.-C. Chen, K.-J. Chen, C.-H. Wang, C.-W. Sher, C.-C. Yeh, C.-C. Lin, C.-H. Chen, and Y.-J. Cheng, "Patterned structure of remote phosphor for phosphor-converted white LEDs," *Opt. Exp.*, vol. 19, no. S4, pp. A930–A936, Jul. 2011.
[11] S. E. Brinkley, N. Pfaff, K. A. Denault, Z. Zhang, H. T. (Bert) Hintzen, R. Seshadri, S. Nakamura, and S. P. DenBaars, "Robust thermal performance of $Sr_2Si_5N_8 : Eu^{2+}$: An efficient red emitting phosphor for light emitting diode based white lighting," *Appl. Phys. Lett.*, vol. 99, no. 24, pp. 241106-1–241106-3, Dec. 2011.
[12] H. Li, H. K. Yang, B. K. Moon, B. C. Choi, J. H. Jeong, K. Jang, H. S. Lee, and S. S. Yi, "Tunable photoluminescence properties of Eu(II)- and Sm(III)-coactivated $Ca_9Y(PO_4)_7$ and energy transfer between Eu(II) and Sm(III)," *Opt. Mater. Exp.*, vol. 2, no. 4, pp. 443–451, Apr. 2012.
[13] *Cree Sets New R&D Performance Record With 254 Lumen-Per-Watt Power LED,* Cree Inc., Durham, NC, USA, 2012. [Online]. Available: http://www.cree.com/news-and-events/cree-news/press-releases/2012/april/120412-254-lumen-per-watt.
[14] H. V. Demir, S. Nizamoglu, T. Erdem, E. Mutlugun, N. Gaponik, and A. Eychmüller, "Quantum dot integrated LEDs using photonic and excitonic color conversion," *Nano Today*, vol. 6, no. 6, pp. 632–647, Dec. 2011.
[15] A. Žukauskas, R. Vaicekauskas, F. Ivanauskas, R. Gaska, and M. S. Shur, "Optimization of white polychromatic semiconductor lamps," *Appl. Phys. Lett.*, vol. 80, no. 2, pp. 234–236, Jan. 2002.
[16] W. A. Thornton, "Luminosity and color-rendering capability of white light," *J. Opt. Soc. Amer.*, vol. 61, no. 9, pp. 1155–1163, Sep. 1971.
[17] A. R. Robertson, "Computation of correlated color temperature and distribution temperature," *J. Opt. Soc. Amer.*, vol. 58, no. 11, pp. 1528–1535, Nov. 1968.
[18] T. Erdem, S. Nizamoglu, X. W. Sun, and H. V. Demir, "A photometric investigation of ultra-efficient LEDs with high color rendering index and high luminous efficacy employing nanocrystal quantum dot luminophores," *Opt. Exp.*, vol. 18, no. 1, pp. 340–347, Jan. 2010.
[19] S. Nizamoglu, T. Erdem, X. W. Sun, and H. V. Demir, "Warm-white light-emitting diodes integrated with colloidal quantum dots for high luminous efficacy and color rendering," *Opt. Lett.*, vol. 35, no. 20, pp. 3372–3374, Oct. 15, 2010.
[20] P. Zhong, G. He, and M. Zhang, "Optimal spectra of white light-emitting diodes using quantum dot nanophosphors," *Opt. Exp.*, vol. 20, no. 8, pp. 9122–9134, Apr. 2012.
[21] K.-J. Chen, H.-C. Chen, M.-H. Shih, C.-H. Wang, M.-Y. Kuo, Y.-C. Yang, C.-C. Lin, and H.-C. Kuo, "The influence of the thermal effect on CdSe/ZnS quantum dots in light-emitting diodes," *J. Lightw. Technol.*, vol. 30, no. 14, pp. 2256–2261, Jul. 2012.
[22] P. F. Smet, A. B. Parmentier, and D. Poelman, "Selecting conversion phosphors for white light-emitting diodes," *J. Electrochem. Soc.*, vol. 158, no. 6, pp. R37–R54, 2011.
[23] Y. Ohno, "Spectral design considerations for white LED color rendering," *Opt. Eng.*, vol. 44, no. 11, pp. 111302-1–111302-9, Nov. 2005.
[24] K. Smet, W. R. Ryckaert, M. R. Pointer, G. Deconinck, and P. Hanselaer, "Optimal colour quality of LED clusters based on memory colours," *Opt. Exp.*, vol. 19, no. 7, pp. 6903–6912, Mar. 2011.
[25] G. X. He and H. F. Yan, "Optimal spectra of the phosphor-coated white LEDs with excellent color rendering property and high luminous efficacy of radiation," *Opt. Exp.*, vol. 19, no. 3, pp. 2519–2529, Jan. 2011.
[26] CIE, "Method of specifying and measuring color rendering properties of light sources," Central Bur. CIE, Vienna, Austria, CIE Publ. No. 13.3, 1995.
[27] W. Davis and Y. Ohno, "Color quality scale," *Opt. Eng.*, vol. 49, no. 3, pp. 033602-1–033602-16, Mar. 2010.
[28] Y. Lin, Y. L. Gao, Y. J. Lu, L. H. Zhu, Y. Zhang, and Z. Chen, "Study of temperature sensitive optical parameters and junction temperature determination of light-emitting diodes," *Appl. Phys. Lett.*, vol. 100, no. 20, pp. 202108-1–202108-4, May 2012.
[29] J. Y. Woo, K. N. Kim, S. Jeong, and C. S. Han, "Thermal behavior of a quantum dot nanocomposite as a color converting material and its application to white LED," *Nanotechnology*, vol. 21, no. 49, pp. 495704-1–495704-8, Dec. 2010.